Joint Institute for VLBI in Europe

VLBI tracking of the Huygens Titan probe
17002/02/NL/LvH/bj, CCN 02
Final report

JIVE Research Note #0005

Version of 18.03.2004

Dwingeloo

This study is conducted at the Joint Institute for VLBI in Europe under CCN 02, Contract between ESA and ASTRON/JIVE No. 17002/02/NL/LvH/bj

Project manager   L.I.Gurvits
Project scientist   S.V.Pogrebenko

Huygens VLBI Tracking Team   I.M.Avruch, H.Bignall, R.M.Campbell, A.Szomoru

Joint Institute for VLBI in Europe
P.O.Box 2
7990 AA Dwingeloo
The Netherlands

Tel: +31-521-596500
Fax: +31-531-596539
e-mail: secretary@jive.nl
        www.jive.nl

Contents

1. Introduction

This report presents the results of the ongoing study of VLBI tracking of the Huygens probe during its parachute descent to the surface of Titan. It continues the study reported earlier (JIVE Research Note #0004 of 2003.07.10, contract No. 17002/02/NL/LvH/bj between the European Space Agency (ESA), and the Netherlands Foundation for Research in Astronomy, ASTRON, and the Joint Institute for VLBI in Europe, JIVE). The goal of the study is to assess the feasibility of detecting and precise tracking of the probe using an Earth-based network of radio telescopes. Such an observation would provide information complementary to Doppler measurements on the trajectory of the probe in the atmosphere of Titan.

This report covers topics as formulated in the corresponding Statement of Work. Section 2 describes observing results and preparation for further radio observations of the "Huygens Field" – the patch of the sky surrounding the position of Titan at the interface epoch (2005.01.14). These include observations using ATCA (Australia Telescope Compact Array, Narrabri, NSW, Australia), WSRT (Westerbork Synthesis Radio Telescope, the Netherlands), VLA (Very Large Array, NM, USA), MERLIN (Multi-Element Radio-Linked Interferometer, UK) and EVN (European VLBI Network).

Development of algorithms and corresponding software for VLBI phase-referencing processing of the Huygens signal is described in Section 3. It contains demonstration results of this software applied to continuum VLBI data obtained with regular EVN observations as well as attempts to detect the signal of the ESA's Mars lander Beagle-2.

Section 4 presents an assessment of the instrumental requirements for Huygens VLBI tracking. It covers availability of radio telescopes, status of S-band receivers, IF analog and digital electronics and data acquisition systems.

Section 5 summarizes conclusions of the present study and outlines the timeline and actions leading to the Huygens VLBI tracking experiment at the interface epoch.

Annex 1 includes some programmatic and logistical details of the project.

Throughout this report relevant parameters of the mission are assumed to be the same as stated in Section 2 of the previous report [1] (JIVE RN #0004 of 2003.07.10).

2. Astronomical reconnaissance of the Huygens Field

As described in the previous report on the Huygens VLBI tracking experiment [1], the Huygens VLBI tracking experiment requires a detailed knowledge of the celestial background field within several degrees of the interface point (the position of Titan at the interface epoch). This field is called the Huygens Field throughout this document. In order to obtain this knowledge, a series of radio astronomical observations of the Huygens Field have been conducted during the period October 2003 – February 2004. Their results are described in this section of the report.

2.1. ATCA observations of the Huygens Field

On 13 November 2003, 6.5 hours of ATCA (Australia Telescope Compact Array) time were used to observe the Huygen's background field as a Target of Opportunity. The observations were made by Bob Sault of ATNF, and used the ATCA's mosaic mode, with 17 pointings covering approximately 1 square degree of sky centered at the interface point. The correlator was used in the standard ATCA continuum observing mode, which comprises two spectral windows, each 128 MHz wide, divided into 8 MHz spectral channels, and gives full polarization parameters. The output data were written using an integration period of 10 seconds. The chosen centre frequencies were initially 2.368 GHz and 2.496 GHz. Partway through the observation, the first frequency was changed to 2.32 GHz as this band was found to be less affected by interference (RFI).

Data reduction was performed using the MIRIAD software package. The flux density scale is tied to the ATCA primary calibrator PKS 1934-638, which was observed for several minutes at the beginning of the observation. PKS 1934-638 was also used to solve for antenna bandpass, initial gain, and polarization leakages. Gain amplitude and phase corrections found using the nearby calibration source J0738+1742, which was observed every 20 minutes, were then applied to all target fields. Phase self-calibration was later performed on a few target fields which contained the strongest sources, using the CLEAN model components. The derived phase corrections were then applied to all other target fields in order to minimise phase errors in the final images. The observed frequencies were affected by RFI, which became more severe as the observations progressed, and substantial clipping of RFI-affected data was required.

All fields were first imaged separately. Data from all frequencies were Fourier transformed together using MIRIAD's multi-frequency synthesis capabilities. The whole primary beam area was imaged for each pointing. MIRIAD's standard CLEAN algorithms were used iteratively for deconvolution, and after convolution with a gaussian restoring beam, a primary beam correction was applied to the final images using MIRIAD's linear mosaicing task. A combined, mosaiced image of the central 7 pointings was also made by Fourier transforming these pointings together, and deconvolving using MIRIAD's mosaic Steer CLEAN algorithm. The rms noise in the final images is limited to typically ~0.3 mJy/beam, which is somewhat higher than the theoretical rms noise, probably mainly due to residual RFI-affected data.

ATCA mosaic image of the Huygens Field at 2.4 GHz obtained in our observations is shown in Fig. 2.1. This mosaic contains 79 compact sources listed in Appendix A.
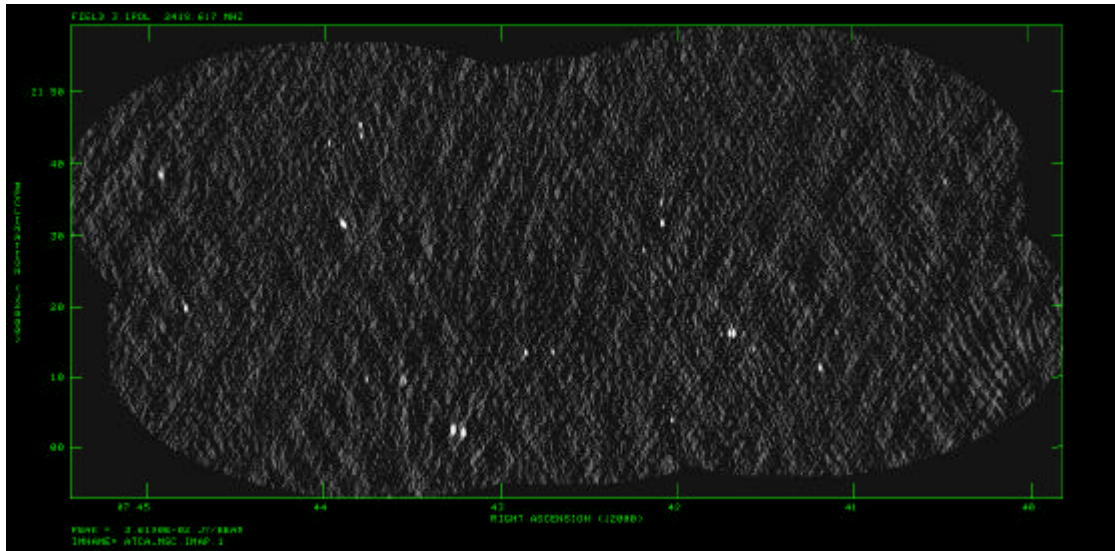

Fig. 2.1. ATCA mosaic image of the Huygens Field at 2.4 GHz. The image is centered on the Huygens interface point. The rms image noise is ~300 μJy/beam, 79 compact sources detected in the field are listed in Appendix A.

2.2. VLA observations of the Huygens Field

On 23 December 2003, the Very Large Array (VLA) observed selected pointings in the Huygens Field for a total of 1.5 hours. With the high sensitivity of the VLA, "snapshot" imaging is possible, wherein the array dwells as little as 90 seconds on each field; this is especially suited to detecting compact sources. Ten pointings of 90 seconds and two of 480 seconds (overlapping the interface point) were performed at both C and X bands (4.9 and 8.4 GHz, respectively). The correlator functioned in normal continuum mode, which gives the user two sub-bands of 50 MHz width around the nominal frequency and all Stokes parameters. The project commenced at 07:05 UTC, and the data were available for FTP to JIVE within seven hours.

Data reduction was performed with the AIPS software package. The source 3C147, a standard flux calibrator for the VLA, was observed for several minutes at each frequency. The source is resolved by the VLA in B configuration, but this was accounted for in processing. A second, unresolved source, J0738+1742, was also observed at each frequency for use as intermediate amplitude and phase calibrator. Two of the 25 antennas failed during the experiment, but otherwise observing conditions were fine and the array produced data of good quality.

For the initial reduction, a map of the full primary beam area was made for each pointing at X band, and followed up at C if a source was detected. After deconvolution (via the standard AIPS CLEAN implementation) and self-calibration, map noise was typically 75

μJy/beam for the central fields, and for the peripheral fields 170 μJy/beam and 210 μJy/beam at X and C bands, respectively; the X band receivers are more sensitive. These values are reasonably close to expectations.

In these data, five compact sources have been detected at both frequencies with apparently flat or inverted spectra and are thus promising targets for VLBI. Two are within 3.43 and 4.63 arcminutes of the interface point, respectively; they are each of flux density ~ 1.5 mJy. Fig. 2.2 shows two examples of VLA images of the Huygens Field compact sources – candidates for phase-reference calibrators for Huygens VLBI tracking. All the VLA detections are noted in the catalog list (Appendix B).
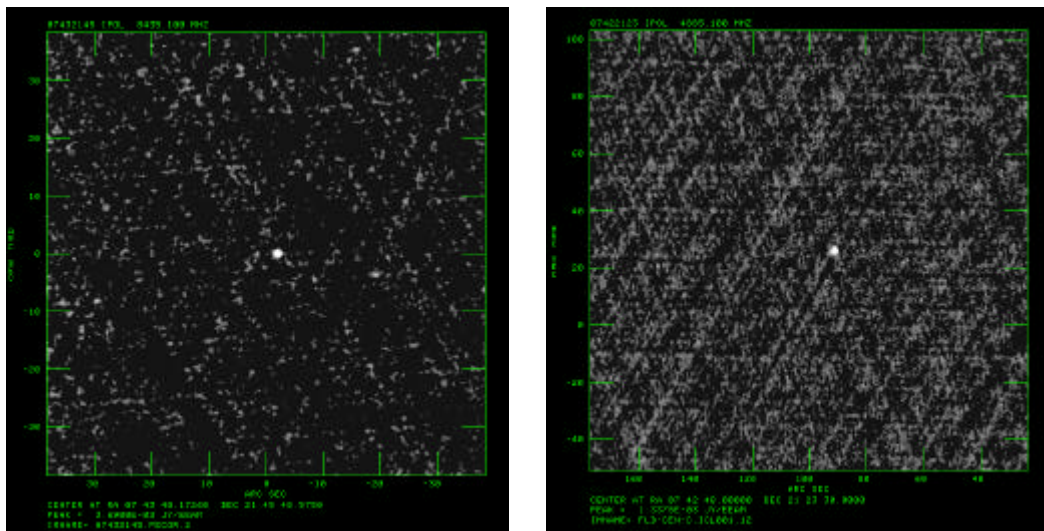
Fig. 2.2. VLA detections of the Huygens Field compact sources: left – J0743+2145 at 8.4 GHz, peak brightness of 3.7 mJy/beam; right – J0742+2123 at 4.8 GHz, peak brightness of 1.3 mJy/beam.

2.3. WSRT observations of the Huygens Field

Westerbork Synthesis Radio Telescope observed the Huygens Field on 30th November 2003 for 7.5 hours, 21st December for 6 hours, 24th December for 3 hours (in the 35 cm UHF band) and on 28th December for 7 hours (at the lower end of the 21 cm band). The 21 cm band observations used 8 sub-bands of 20 MHz each, with the standard 64 channels per sub-band.

The data were reduced using the NEWSTAR software package. Flux density and bandpass calibration were based on the primary calibrator 3C286, and phase calibration was checked using the nearby point source PKS 0745+241. Some of the data were affected by RFI and must be removed before accurate high-dynamic range images can be made. Wide-field maps made over the wide fractional bandwidth (10% at 800 MHz) must use the bandwidth synthesis technique, so the data cannot be averaged over frequency, nor can they be averaged over time as the data were observed in mosaics. These facts combine to make the datasets several gigabytes in size.

After flagging of RFI in the unprotected UHF band, the data have been fully calibrated and mapped. The images show some unresolved sources at the Westerbork resolution (about 15 arcseconds in the UHF band), and allow derivation of flux densities and, in combination with observations at other frequencies, spectral indices of the closest radio sources to the interface point. Spectral indices are used as an indicator of source compactness and suitability for use as VLBI phase references. See Appendix B for a partial list of WSRT detections.

2.4. MERLIN observations of the Huygens Field

During the weekends of 8th–9th and 15th–16th November 2003, observations of potential phase reference calibrators near the Huygens Field were performed with the MERLIN array in the UK using director's discretionary time. The sources were chosen based upon the ATCA, WSRT, and VLA results: sources that were promising calibrators or yet unobserved were scheduled. Some telescopes were under maintenance, so the array consisted of only four stations, therefore the image fidelity was reduced, but that does not affect the detectability of point sources, provided they are sufficiently bright. Observations of 21 sources were conducted at C-band (6 cm), and eleven had sufficiently high surface brightness to be detected. We also note that MERLIN data provide accurate astrometry positions on the sources – a crucial input for further VLBI observations. Positions and flux densities are listed in Appendix B, and examples of MERLIN images are shown in Fig. 2.3.

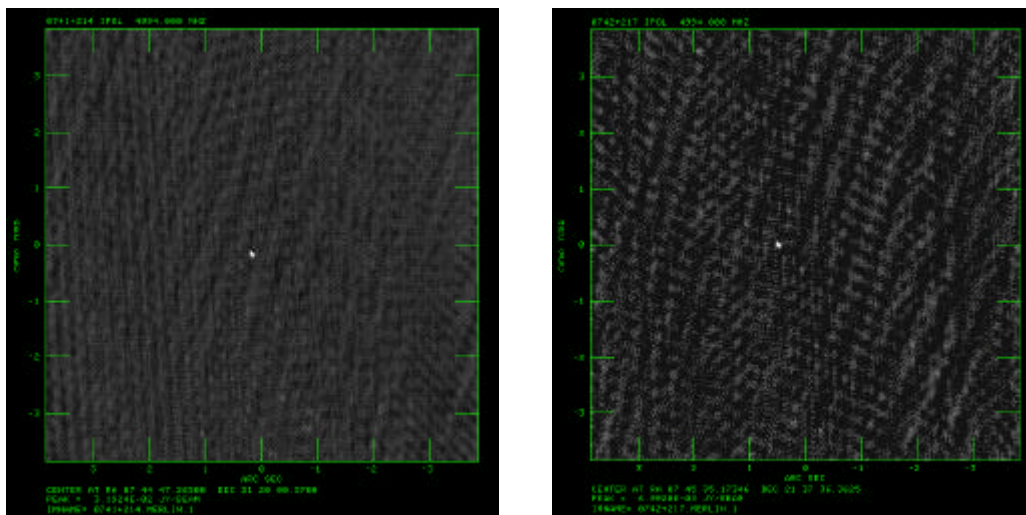*Fig. 2.3.* Examples of MERLIN images of potential phase-referencing calibrators in the Huygens Field at 6 cm: left – 0741+214, peak brightness of 32 mJy/beam; right 0742+217, peak brightness of 7 mJy/beam.

We will shortly re-observe with MERLIN several of the most promising sources in a more complete configuration in the first-second quarter of 2004, providing better imaging fidelity and higher signal-to-noise.

2.5. EVN observations of the Huygens Field

On February 19th 2004, the European VLBI Network observed the Huygens Field and nearby sources which are promising phase reference calibrators for Huygens VLBI tracking. The experiment was conducted at L-band (18 cm), the most sensitive frequency of the array. Over a period of four hours, nine telescopes spread geographically from China and South Africa to Europe, observed four radio sources in and near the Huygens Field in phase-referencing mode. The known bright, compact source 0735+178 was used as fringe finder. A source less bright but still compact, J0735+2036, was used as a primary phase calibrator. The telescopes slewed between the primary phase calibrator and the four other fields in an interleaved pattern.

The observational data were recorded on Mk5 disk-based VLBI recorders at most of the stations, subject to availability; the stations in China (Nanshan and Sheshan) and South Africa (Hartebeesthoek) recorded on Mk4 tape. The experiment appears to have been a success, based on the observation logs from the stations. The 76-m Lovell Telescope at Jodrell Bank had a technical problem with the Mk5 unit that under normal circumstances would mean the loss of all data from that station. However, with the software developed as part of the Huygens processing toolkit, we expect to recover half the observed data from Lovell, which is fortunate because it is the most sensitive station in the array.

The data disks and tapes have all arrived at the EVN Data Processor at JIVE in Dwingeloo and await checkout and correlation, probably commencing before the end of March, 2004.

2.6. Summary of radio astronomy observations of the Huygens Field

Results of the observations described in this section allow us to conclude that the composition of celestial radio sources in the Field is suitable for Huygens VLBI tracking. Flux densities of the sources in the field are considerably lower than in routine VLBI observations. It poses a certain challenge. But with the advanced characteristics of the Mk5 recording system and state-of-the-art wide-band Mk4 VLBI correlator at JIVE and narrow-band software VLBI toolkit developed for the Huygens project, the goal of tracking the Huygens Probe can be achieved. A summary on sources detected in the Huygens Field in ATCA, WSRT, VLA and MERLIN observations described in this report is presented in Appendices A and B.

3. VLBI processing of the Huygens signal: algorithms, software implementation and test examples

The architecture of the Huygens probe VLBI data processing is based on an extension of the EVN Mk4 correlator at JIVE [2].

It is essential for the project that signals from both the probe and the calibrators are recorded onto the same standard VLBI recording medium. Mk5 disk-based VLBI recorder/playback units [3], which are currently in use at some of the EVN and IVS VLBI stations, are capable of recording radio signals at a data rate of up to 1 Gbps for several hours. The K5 system used in Japan has similar characteristics. Tools for data exchange between Mk5 and K5 units have been developed at CRL (Japan) [4].

The EVN Mk4/Mk5 VLBI data processor at JIVE (aka JIVE Mk4 VLBI correlator) is currently equipped with 16 Mk4 tape-based playback units and 4 fully operational Mk5 disk based units. Two more Mk5 units are in the process of system integration. The correlator itself is capable of processing 256 MHz bandwidth of data from up to 16 VLBI stations simultaneously; mixed tape/disk playback and processing is also possible, although disks are preferable. Fig. 3.1 shows the block diagram of the EVN correlator data/control flow and its extension for the Huygens probe signal processing.
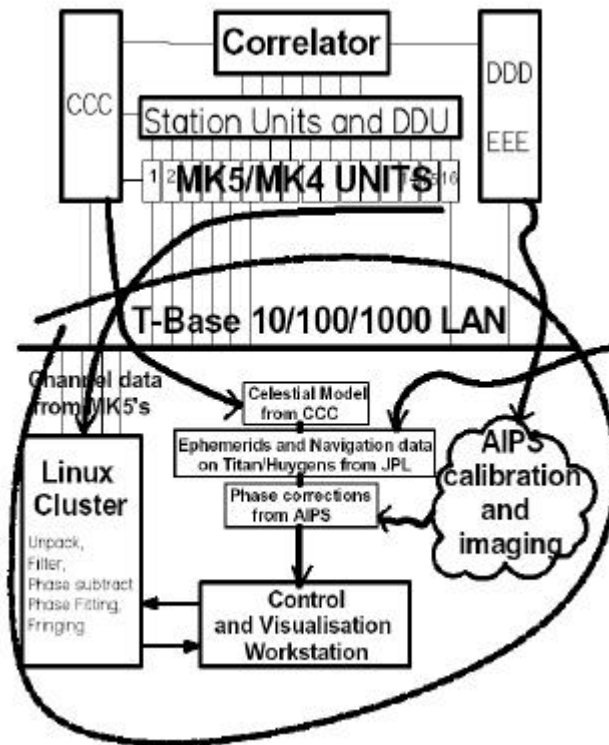

Fig.3.1. Block diagram of the EVN correlator at JIVE (at top) and its extension for the Huygens signal processing (encircled area at the bottom).

It is a challenging task to process both the narrow band data from the Huygens probe and the broad-band data from phase calibration radio sources with adequate accuracy and mutual phase coherence. At a full bandwidth of 256 MHz and 16 stations, the JIVE correlator is able to achieve spectral resolution of the order of 100 KHz (with a reasonable number of data passes), while for the probe detection we need something 5-6 orders of magnitude better, although in a much narrower total bandwidth.

A possible solutions is to download a 16 MHz-wide channel of data from Mk5 units into a powerful general purpose computer, i.e. a Linux cluster, filter the bandwidth down to a level acceptable from the point of view of initial Doppler shift uncertainties, and then process it in a phase referencing spectroscopic VLBI mode. The required spectral resolution of ~1 Hz for primary detection with the biggest radio telescopes and ~10 mHz resolution for final tracking on all the stations is then a matter of proper software implementation.

Within this architectural solution, the processing algorithm is as follows:

1. Correlate the calibrators' broad-band signals using the JIVE correlator with a standard setup.
2. Fringe-fit, calibrate and map the calibrators' data using the Astronomical Image Processing System (AIPS) software. Obtain a phase correction model for each radio telescope.
3. Download of the 16 MHz channel data from Mk5 units to the Linux cluster.
4. Apply a nominal geocentric Doppler-shift model based on the JPL ephemeris of Titan motion. Filter down the bandwidth of data to about 10 kHz corresponding to +/- 600 m/s velocity uncertainty. Apply the nominal telescope motion models, narrowing down the bandwidth to 4 KHz or +/- 300 m/s, which will cover the most extreme motion model residuals.
5. Apply the multitude of possible probe trajectories, based on different atmospheric and parachute performance models with a residual uncertainty of about 5-10 m/s. That will allow us to see the signal on dynamic spectra from the largest (100 to 64 m diameter) telescopes.
6. Phase-lock the motion model to the detection, applying the individual telescope phase corrections derived from calibrators' images, narrowing down the bandwidth to about 10 Hz and frequency resolution to about 50 mHz, and confirming the visibility of the signal at 25–30-m class antennas. At a frequency resolution of $\delta F > 30$–40 mHz, there will be no significant phase difference between data from different telescopes, so only the radial velocity model, common for all the telescopes, needs to be applied.
7. Fit a model of 3-dimensional motion, consider the differential phases between telescopes caused by tangential motion of the probe, and include more telescopes into the analysis. Phase fitting can run iteratively in a loop to improve the frequency resolution and SNR until the final accuracy is achieved.

We have implemented this algorithm in a software model and performed several tests during the development of various parts of these algorithms and software tools. The following subsections describe the software model tools and present results of the tests.

3.1. Handling the Mk5 data

Handling the Mk5 data and converting them into a format acceptable by general-purpose software is a considerable programming task, indeed the most CPU-time consuming task of the software toolkit developed and tested so far for the Huygens VLBI project.

This task includes several sub-tasks:
1. Data transfer from Mk5 to a general purpose computer;
2. Synchronization to the imbedded time stamps;
3. Unpacking the bit-wise coded data samples and reconstructing base-band signals.

We exercised two methods of data transfer. The first one involved copying data from a Mk5 disk-pack into the system disk and then transferring the file to the software correlator PC by FTP. The second method was to copy data directly into a transportable USB disk and then connect this disk to the software correlator PC. The second method was found to be considerably faster, although the data transfer still required several times more time than the duration of observation. Use of advanced technologies such as an SCSI or IDE RAID directly mounted over Gigabit Ethernet can improve the performance of data transfer.

Synchronization of data processing to the Mk5 time stamps is another essential part of data handling software. Fig. 3.2 illustrates a piece of code and a display of the synchronization process. The software finds sync-words, decodes time stamps, and starts data processing from the first whole second in the data file. The decoded time stamp (day, hour, minute, second and millisecond of the start segment of data) is displayed on the right side of sync-word display.

$$\text{FATA} := \text{READBIN}(\text{INPFILE}, \text{"byte"}, 0, 8, \text{skip2start}, \text{Nfata})$$

$$\text{synch} := \text{synchdet}(\text{FATA}) \quad \text{jsy} := 0 .. \text{length}(\text{synch}) - 1 \quad \max(\text{synch}) = 1 \quad \text{synx} := \text{fsynch}(\text{synch})$$

$$\text{synx} = 64 \qquad \text{length}(\text{synch}) = 79969 \quad \text{jtcd} := 0..51 \qquad \text{TCD}_{jtcd} := \frac{1}{255} \text{FATA}_{\text{synx}+32+\text{jtcd}, 0}$$

SYNC WORD DISPLAY
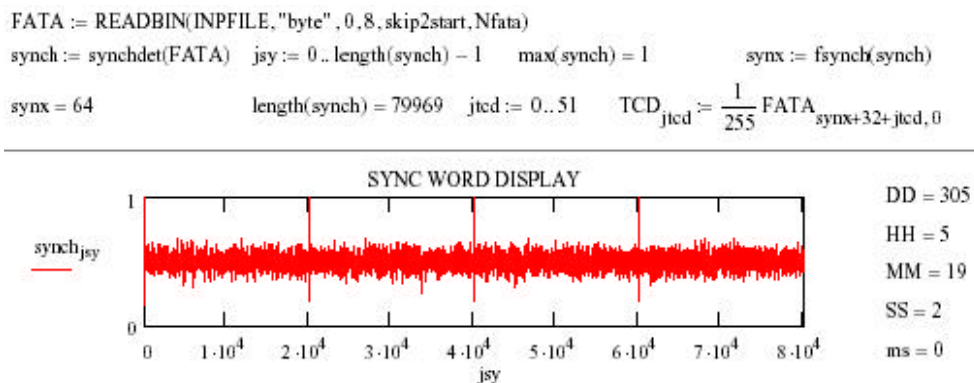
DD = 305
HH = 5
MM = 19
SS = 2
ms = 0

Fig. 3.2. Data synchronization display. High spikes on the plot correspond to the sync-words of Mk5 data frame format; time stamp of the first sync-word is displayed at the right side of the plot.

Proper unpacking and decoding of Mk5 bit-streams is checked by a track identification routine based on the MkIV format specification [5]. Fig. 3.3 presents the results of track ID decoding – extracted codes for BBC number, USB/LSB ID, and sign/magnitude assignment of bit streams.
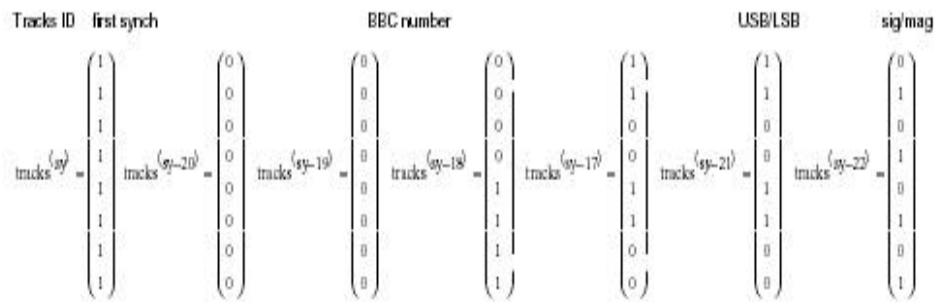
Fig. 3.3. Mk5 bit-stream ID display

Base-band data are reconstructed from sign and magnitude bits using weight ratio 3:1 for magnitude 'high' to magnitude 'low', the same as for the standard MkIV VLBI hardware correlator, although the multiplication scheme for software processing includes all possible products.

Finally, after re-assembling the base-band signals from sign and magnitude bits, the Mk5 headers are replaced with Gaussian noise, so the base-band data is ready for spectral analysis and digital filtering.

3.2. Ultra-high spectral resolution correlation test

We have performed this test in order to check the data consistency when transferring raw VLBI data from a Mk5 unit and control parameters (telescope motion models) from the MkIV Correlator Control Computer (CCC) into a general-purpose computer, running a specially designed ultra-high spectral resolution software correlator. The spectral resolution of 8 Hz (1 million spectral bins, or equivalent of 2 million lags) achieved over the 8 MHz band is close to that required for detecting the Huygens probe's signal. Fig. 3.4 illustrates the test correlation results for the radio source DA193 with the flux density of 5 Jy at 5 GHz on the EVN baseline Effelsberg–Medicina, observed on 02.06.2003 and processed on 27.09.2003. Comparison of the achieved SNR with the SNR obtained during the standard processing with the EVN correlator shows perfect consistency.
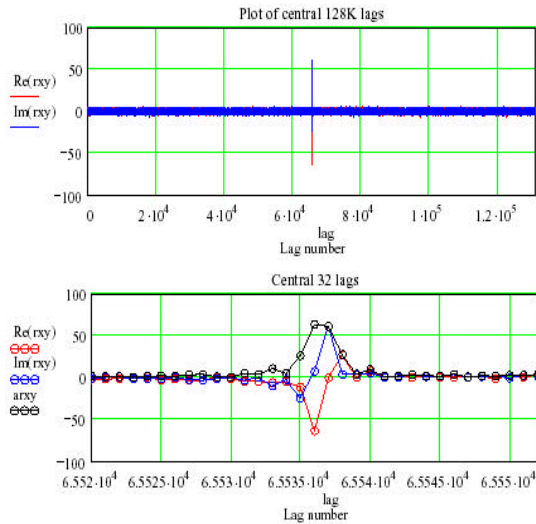
Fig. 3.4. VLBI response (cross-correlation function) of the ultra-high spectral resolution software correlator.

3.3. Application of the Huygens VLBI Project Software to the Ultra High Spectral Resolution Analysis of VLBI Phase Calibration Tones

High spectral resolution analysis of the phase calibration tones of several EVN radio telescopes was prompted by a malfunction of the C-band front-end local oscillator at the Lovell telescope (Jodrell Bank radio observatory) during the November 2003 EVN VLBI session.

We use this example as a demonstration of the application of the Huygens project software to real VLBI data recorded with the use of disk-based Mk5 units.

Fig. 3.5 presents a simplified block diagram of the RF signal processing setup of a typical VLBI station. Phase calibration tones are locked to the same hydrogen maser as the front-end and back-end local oscillators, and propagate through the same RF data path as the signals from external radio sources. Normally the phase-cal tone is used to align the phases between different base bands, but it is also a tool for checking signal coherency through all sections along the RF data path.
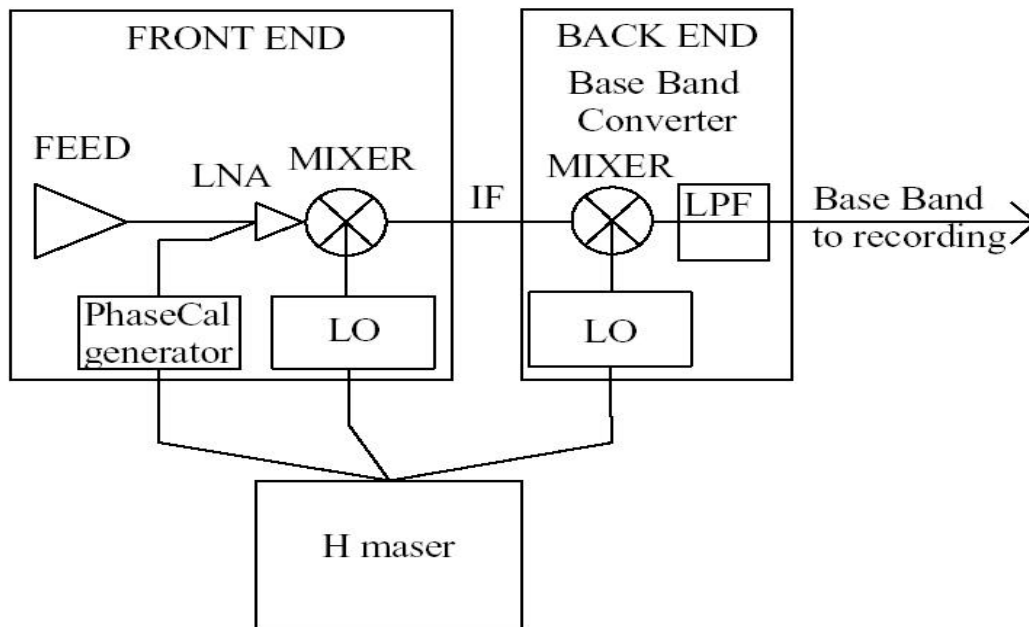
Fig. 3.5. Simplified block diagram of a typical RF data processing setup at VLBI station.

Phase-cal tones normally form a 1 MHz grid over the whole RF band. Fig. 3.6 illustrates the phase-cal tone distribution across an 8 MHz span of lower and upper side bands with 30 Hz resolution, and integration time of 32 ms (data from D03C3 EVN NME scan, station Effelsberg).
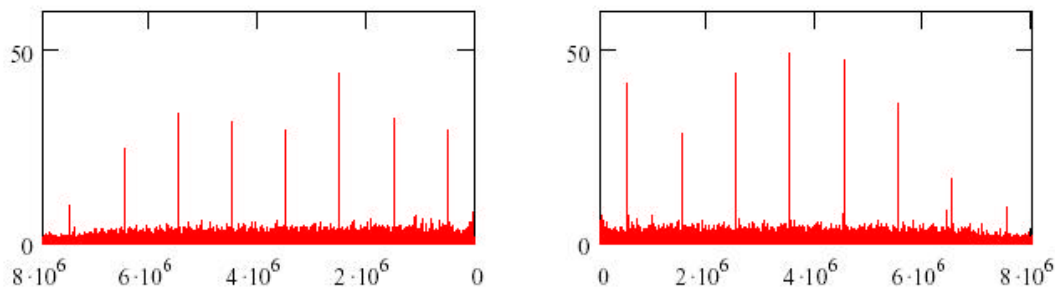
Fig. 3.6. An example of phase-cal tones in the lower and upper side bands.

During the correlation of the observational data from the November 2003 VLBI session at the EVN correlator at JIVE and the VLBA correlator in Soccoro, it was found that the correlation functions of all the stations against the Jodrell Bank Lovell 76-m telescope showed strange behavior at C-band, with sporadic appearance and disappearance of the correlation. It was suspected that the front-end LO of the Lovell telescope was not properly locked to the hydrogen maser. For a better diagnostic of the event, we performed a high spectral resolution analysis of the phase-cal tones for several EVN stations using the Huygens VLBI project software toolkit.

For this analysis we used 13 seconds of Mk5 data recorded at 256 Mbps, from observations conducted at C-band (5 GHz), with 8 base bands of 8 MHz bandwidth each from Onsala, Effelsberg, Medicina and Jodrell Bank stations. These were sent to JIVE from the telescopes during the network monitoring experiment D03C3 on 02 11 2003.

These data were downloaded to the Huygens project software platform. After unpacking the Mk5 data, 1 kHz bands around the first phase-cal tone in one of the base bands were filtered down and then processed with high spectral resolution. In this case we used 1 second-long data segments, overlapping by 75%, so the sampling for individual spectra was 4 times per second. Because the amplitude of the phase cal tone in the 1 kHz band is sufficiently high, we applied a super-resolution of 1:16, padding the 2K samples of data with zeros to 32K length, so dynamic spectra have about 1 Hz native spectral resolution and 0.06 Hz super-resolution, which is possible due to the high signal-to-noise ratio. Fig. 3.7 illustrates the sampling of the data in the time domain, in full time span and zoomed to a 0.1 second span. In a band of 1 kHz width the strength of the phase-cal tone provides about a 20:1 signal-to-noise ratio.
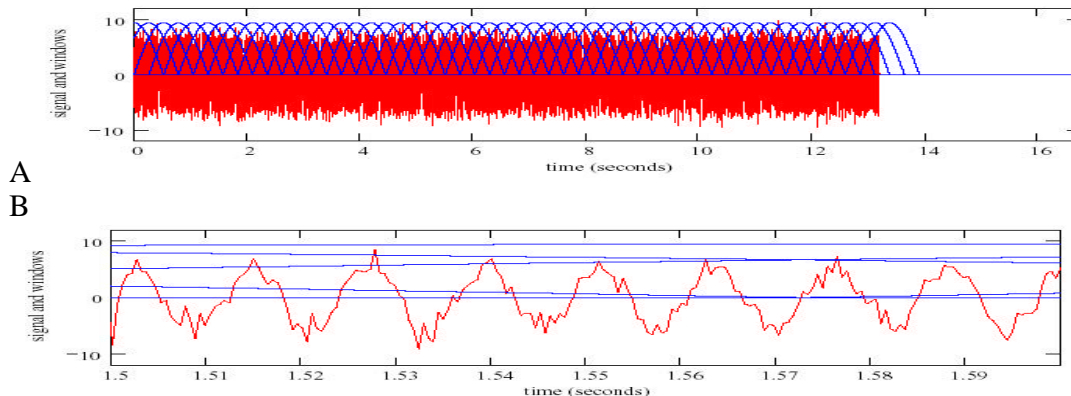
Fig.3.7 Time domain sampling of the data for the dynamic spectral analysis in a 1 KHz band. Signal: red; time domain windows: blue. Time span 16.5 s (A), zoomed span 0.1 s (B). Data from D03C3 EVN NME scan, station Jodrell Bank.

After sampling and windowing, the 1 kHz data were processed to obtain dynamic spectra. Fig. 3.8 presents the dynamic spectra of phase-cal tones for two stations – Medicina (left) and Jodrell Bank (right). The Medicina data were used as reference and showed a stable monochromatic tone, while the phase-cal tone in the Jodrell data (with the malfunctioning LO) exhibits a typical random walk pattern in the frequency domain with deviations +/- 2 Hz on a time scale of several seconds.

It is worth mentioning that such the signal frequency behavior in the case of the Huygens probe would correspond to a Doppler shift amplitude of about 30 cm/s on a time scale of 5 s, corresponding to the extreme values expected from the coning or penduling of the probe during descent [6]. In the case of penduling, it will correspond to ~1 m amplitude with a ~10 second period.
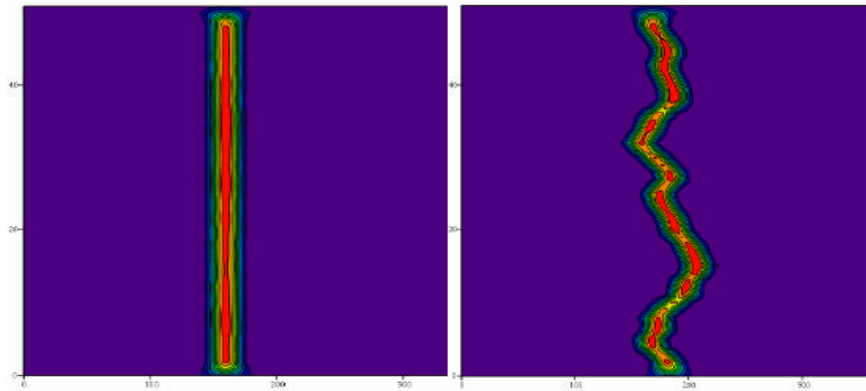
Fig. 3.8. Dynamic spectra of phase calibration tones for Medicina (left) and Jodrell Bank (right) of the D03C3 NME data set. Horizontal axis: frequency, span 20 Hz, sampling 0.06 Hz. Vertical axis: time, span 13 s, sampling 0.25 s.

The same analysis was performed on data from Onsala and Effelsberg. Results show the same monochromatic behavior of phase-cal tone as it is illustrated by Medicina data.
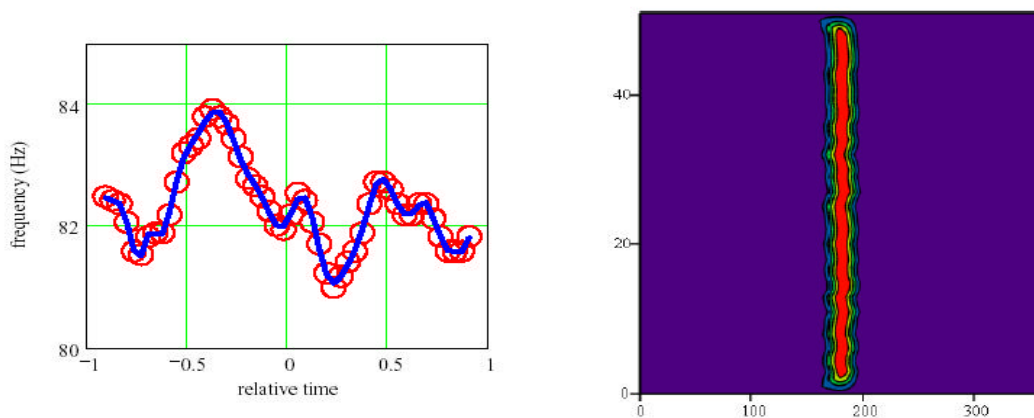
Fig.3.9. Frequency behavior detections (red circles) and polynomial fit (blue line) (left) and dynamic spectrum of the Jodrell Bank phase calibration tone after the phase correction was applied (right).

We used this opportunity to check another aspect of the Huygens software: the phase extraction and correction algorithm proposed in [1, 7], on real Mk5 data. Frequency curve detection was exercised on the dynamic spectrum. After that, this curve was fitted with a 30-th order Chebishev polynomial, and the phase curve was reconstructed as an integral of the frequency curve over time. Phase correction was applied to the raw 1 kHz data and the dynamic spectrum was recalculated. The effective performance of this algorithm shown on the simulated data [1, 7] has now been confirmed with real data, although there still remains an SNR issue.

Fig.3.9 presents the result achieved after a single iteration of this exercise: the frequency curve detections, the polynomial fit plot and the dynamic spectrum of the phase-cal signal after the 1 kHz filtered base band data was corrected for the instability of the local oscillator.

The ultimate check on the accuracy of the frequency/phase behavior curve extraction and correction can be performed with a full length / full spectral resolution spectrum. Comparison of the reference 0.06 Hz resolution spectrum of the phase-cal tone from Medicina station with that from Jodrell Bank, before and after phase correction, is shown in Fig.3.10. As can be seen, the effective width of the tone of the corrected Jodrell Bank data has narrowed to less than 0.1 Hz (from the original 3 Hz span) and the residual phase deviations can be considered as a random walk in the phase domain rather than in frequency domain, as it was before the correction.

Fig.3.10. Full 60 mHz resolution spectra of 13 seconds of data samples from Medicina (A), Jodrell Bank uncorrected (B) and Jodrell Bank corrected (C).

3.4. The WSRT observations of the Beagle 2 Mars lander

3.4.1. *Observations*

The WSRT observations of Mars were carried out at UHF band on 26 12 2003, in parallel with similar observations at Jodrell Bank, in an attempt to detect a signal from the

Beagle 2 Mars lander. The expected frequency of the signal was 401.565344 MHz (corrected for topocentric Doppler shift). At the expected 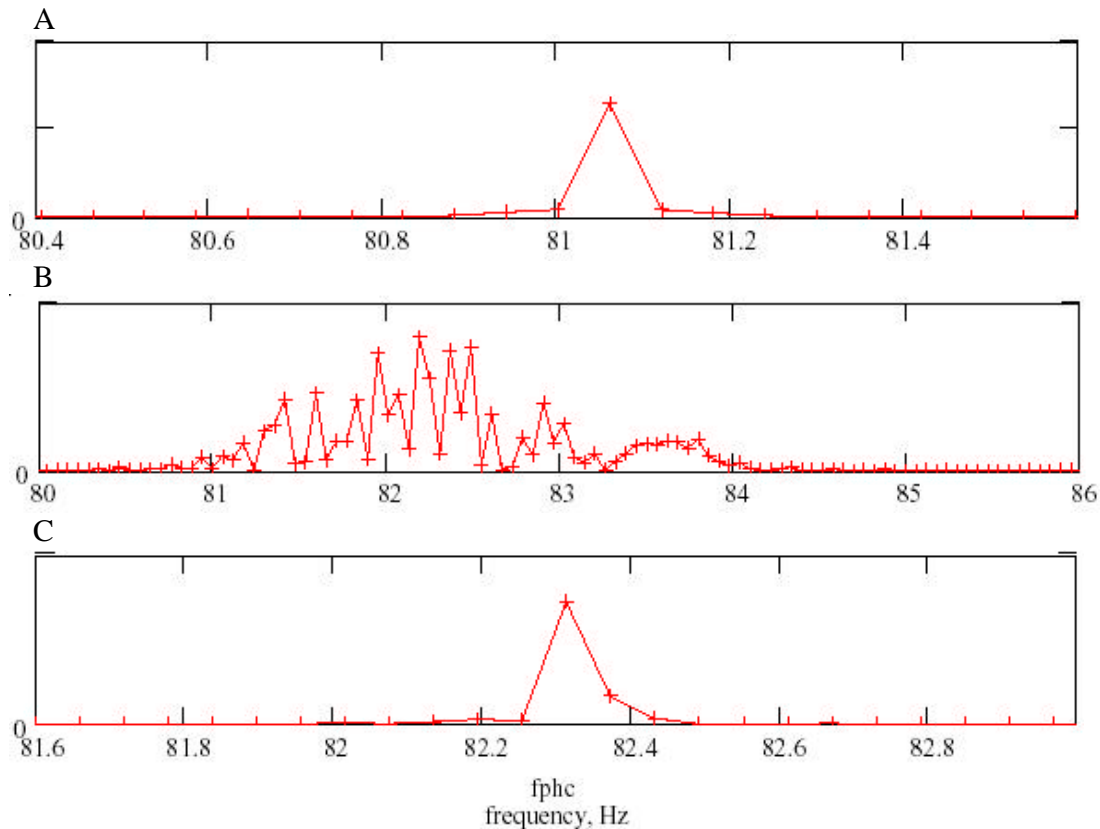time of the signal reception at Earth (22h 50m – 23h 05m UTC) Mars was rather low on the horizon, 9-7 degrees, just at the limit of visibility for the WSRT. Moreover, the spectral region around 401 MHz was severely affected by RFI from mobile telecommunications.

During observations, the WSRT was used in tied array mode and the data acquisition system was configured for two polarisations, LCP and RCP, and two sidebands, LSB and USB, each with 4 MHz bandwidth. Data were recorded on a Mk5 unit at 64 Mbps.

3.4.2. *Data Processing*

The day following the observations, data were copied from the Mk5 disk pack onto a portable USB disk.; the copying process took 2.5 hours for 15 minutes of observed data.

The observational data were then processed with software developed for the Huygens project. First, both USB and LSB were processed with low spectral resolution (16K frequency bins over 4 MHz, or 60 Hz resolution) averaged for 10 seconds, to get an impression of the RFI situation. Full bandwidth 60 Hz resolution spectra are shown in Fig.3.11. Strong RFI peaks have a level 10-15 dB above the continuum, although it's possible that the continuum itself was formed not by thermal noise but by broadband RFI.
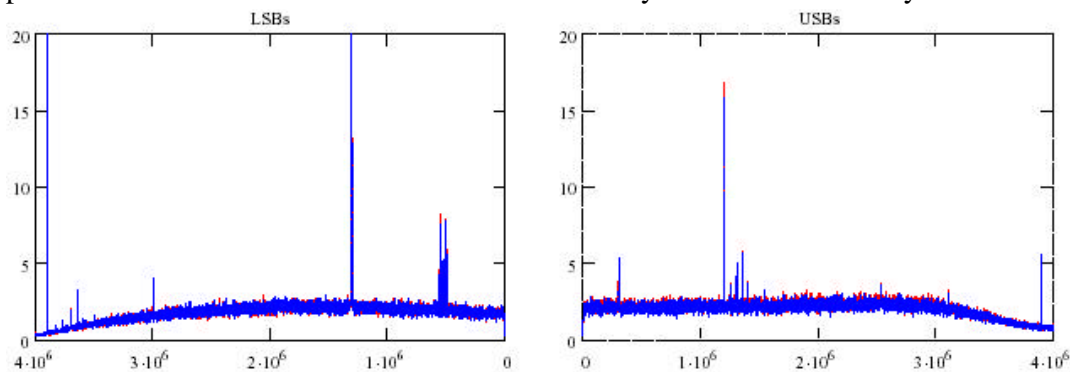
Fig.3.11. Averaged 60 Hz resolution spectra for both polarizations (LCP – red, RCP – blue) and both sidebands (LSB – left, USB – right).

We expected the Beagle signal within a 2.5 MHz region in LSB, which was rather free from at least strong narrow band RFI.

The next step was to process LSB data for both polarizations, focusing attention on a frequency region around the expected 401.565 MHz signal with better spectral resolution and for a longer time span. We selected 8 Hz resolution for this stage of processing because the expected jitter of the Beagle onboard oscillator was about 2 Hz.

Processing of all 15 minutes of data for two polarizations with 8 Hz resolution on a 2.8 GHz P4 platform took 50 hours of computer time and was finished on the 5th of January 2004. A dynamic spectrum of the 4 kHz wide frequency region around the expected signal is shown in Fig.3.12.

3.4.3. *Data Analysis*

No significant spectral or temporal features are seen immediately on the dynamic spectra. Fig.3.13 presents global averages (over all 15 minutes) of the dynamic spectra for both polarizations. The SNR for the maximum spectral features of these averaged spectra is below 3 sigma.
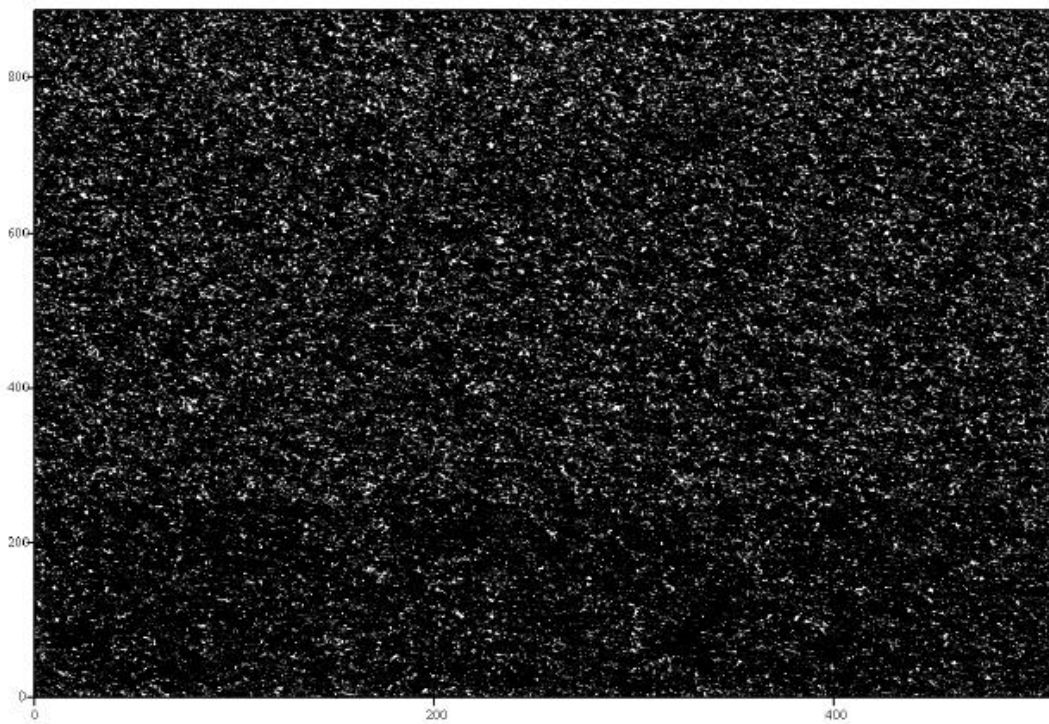
Fig. 3.12. Dynamic spectrum of 4 kHz band around the expected signal location (which is in the central bin). Horizontal axis: 512 frequency bins, 8 Hz per bin. Vertical axis: time, 15 minutes span, 1 s sampling,. Polarization: RCP.
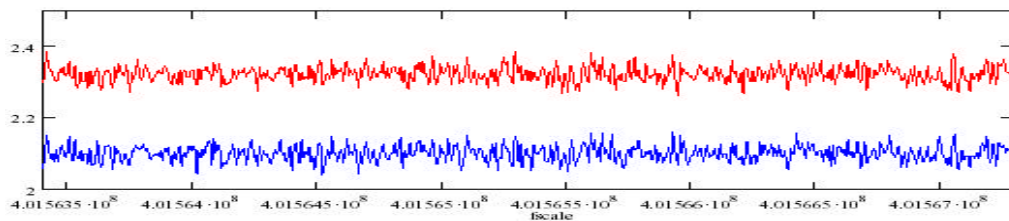
Fig. 3.13. Global average spectra for both polarisations. Frequency span - 4 kHz.

For further analysis we used knowledge of the temporal character of the transmission. It was expected that the lander will transmit the data in 10 second-long bursts each minute. To search for such the temporal signature in the dynamic spectrum we built a set of

optimal filters. Fig. 3.14 (top) presents the plots of time domain prototypes of 1 min periodic pulses with 1:5 duty cycles and lengths in a range from 6 to 10 minutes. Spectral shapes of these filters are shown in Fig. 3.14 (bottom) overlaid on the spectrum of "power output" of the dynamic spectrum for each frequency bin.
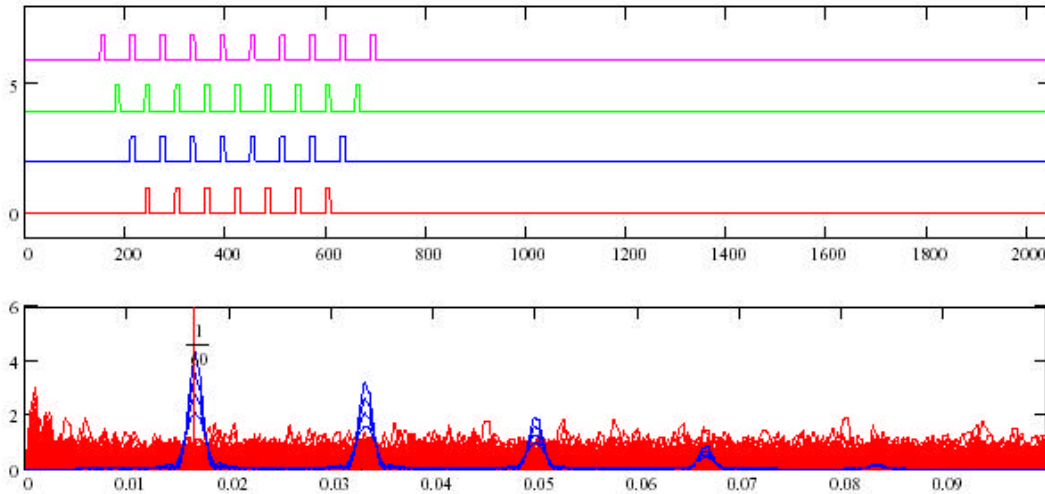
Fig. 3.14. Time domain prototypes and spectral shapes of the optimal filters for the search of 1 minute periodicity in the dynamic spectrum.

The most significant detections with these filters are shown in Fig.3.15. These detections are normalized by the global RMS of outputs for all the filters.
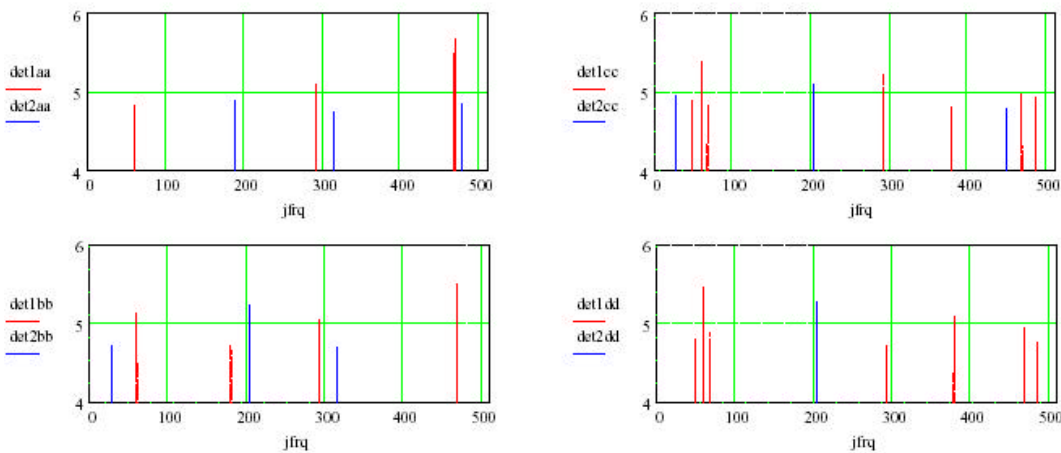
Fig. 3.15. Optimal filter detections for different models.

The temporal behaviour of these detections is shown in Fig.3.16. The one at ordinate 11 has the maximal SNR of 5.8 and shows the distinguishing 1 min periodicity of pulses with the right duty cycle. An overlay of this pattern on the row data from the same frequency bin is shown in Fig.3.17 (top) and can be considered a true detection. Zoomed

view on the temporal behaviour of this signal for both polarizations (Fig. 3.17 bottom) shows that there is a strong correlation between both polarizations over the full time span, both for times when the signal is supposed to be ON as well as when it is supposed to be OFF.
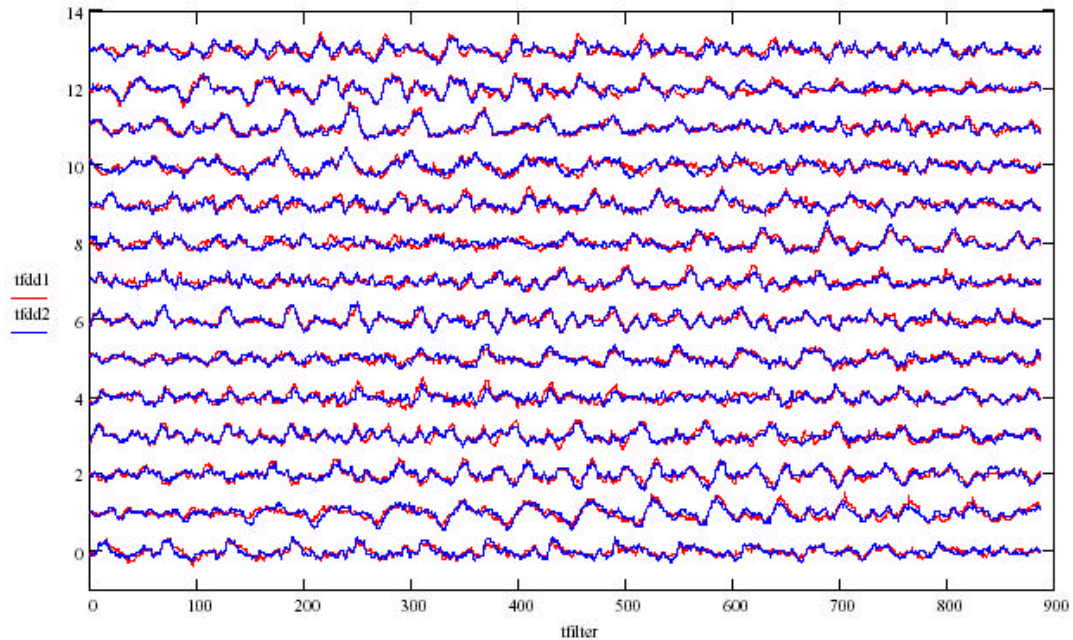
Fig. 3.16. Temporal behaviour of the most significant outputs of optimal filters.
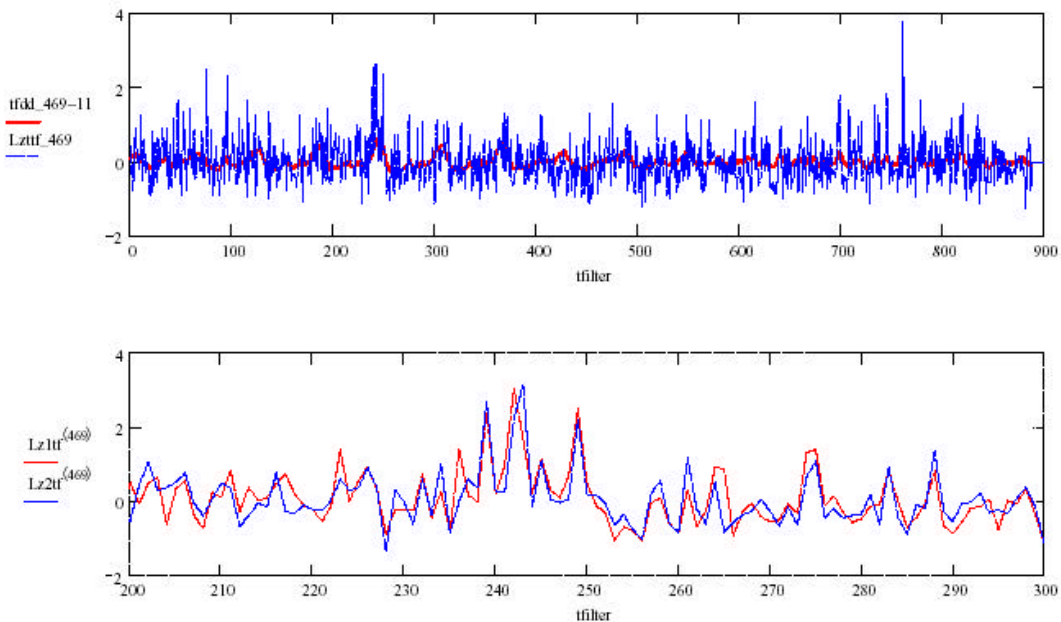
Fig. 3.17. Overlay of the most significant 1 minute periodic detection over the row data of the corresponding frequency bin of the dynamic spectrum (top) and zoomed view on the temporal behaviour of this frequency bin over 100 seconds for both polarizations.

Such a correlation between two circular polarizations leads to the most likely explanation: this signal is linearly polarized, shows 1 minute periodicity and is generated by terrestrial telecommunication equipment.

3.5. Summary of the Huygens software model toolkit tests.

The tests described above allow us to conclude that the Huygens VLBI project software model toolkit can:

1. handle real Mk5 VLBI data in volumes comparable with that of Huygens VLBI tracking observations;
2. convert Mk5 files into files acceptable by general purpose software platforms;
3. synchronize both time and frequency scales with those embedded in Mk5 data;
4. perform digital filtering of broad-band Mk5 data to a kHz level;
5. perform a spectral analysis with a resolution from tens of Hz to tens of mHz;
6. extract frequency/phase behavior curves for narrow band signals with good SNR;
7. perform high-order polynomial phase corrections to remove the detectable frequency/phase deviations although still has to be tested at a lower SNR and different frequency/phase deviation models.

The software model toolkit was implemented on a high-level mathematical language platform – the MathCAD-11 software. This model can run on a single-CPU computer only. Implementation of the operational Huygens VLBI tracking software on a multi-processor platform and appropriate programming language will require considerable efforts (see Annex 1). However, such the migration to the multi-processor platform is inevitable in view of large amount of data to be obtained in "live" Hugens VLBI observations.

4. Instrumental and preparatory requirements of the Huygens VLBI tracking experiment

4.1. Radio telescopes, receivers and data acquisition systems

At the interface time, Titan will culminate over Eastern Pacific, North of the Equator. This requires to choose telescopes in North America and the Pacific Rim area. Table 4.1 includes telescopes – potential participants of the Huygens VLBI tracking experiment in that suitable geographical area, and Fig. 4.1 illustrates visibility of Titan from some of them. We note, that NASA DSN antennas in Goldstone (CA, USA) and Tidbinbilla (ACT, Australia) as well as the ESA Tracking Station in New Norcia are not included in the Table since at the time of this writing their availability for the Huygens VLBI tracking was unlikely. However, if this situation changes, their participation in the experiment would be valuable.
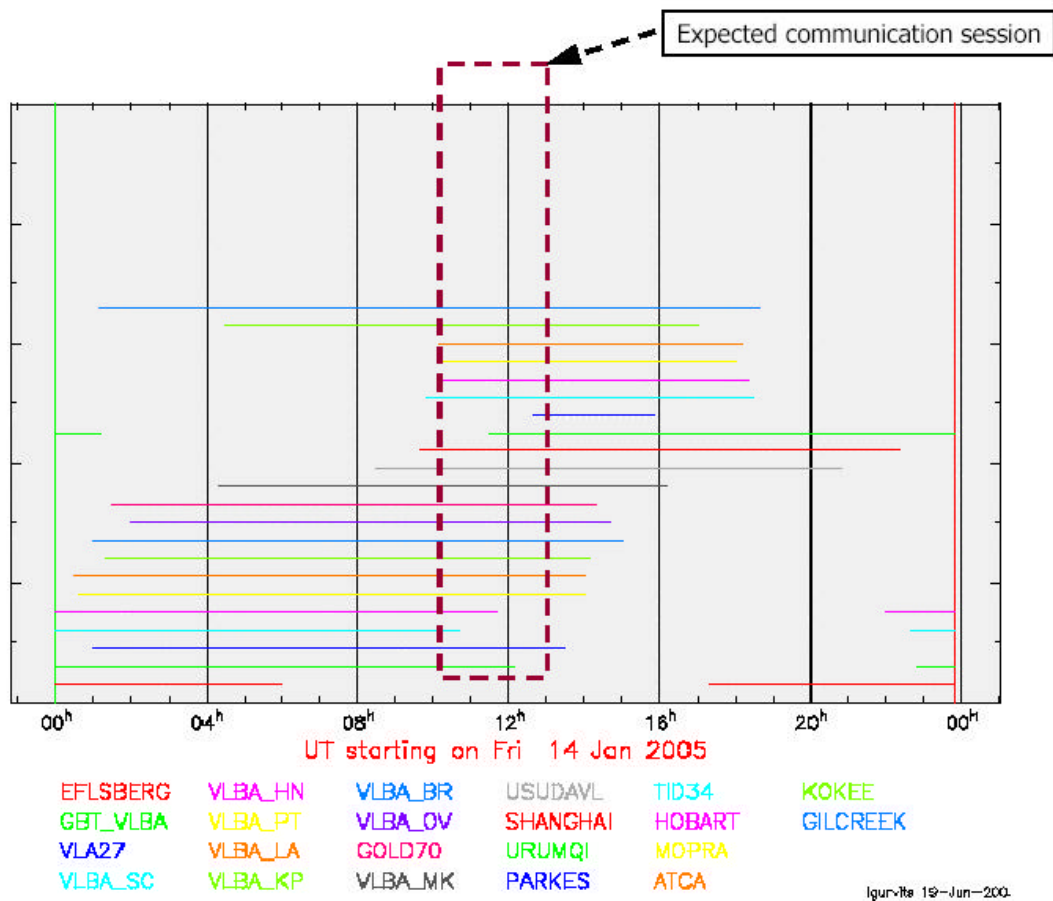
Fig. 4.1. Visibility of Titan at the interface epoch from various radio telescopes (color-coded according to the list in the bottom part of the plot).

Assuming the nominal interface time, the probe observations must start at ~10:00 UT on 14 Jan 2005 and last for at least 2.5 hours. This, together with other factors (e.g.

availability of appropriate S-band receivers) narrows the choice of telescopes to those twenty listed in Table 4.1.

Table 4.1. Radio telescopes – potential participants of the Huygens VLBI tracking experiment.

	Telescope	Country	Diameter [m]	T_{sys} [K]	Eff	Status S-band Rx	Mk5
1.	GBT	USA	100	23	0.71	OK	Need
2.	VLBA_SC	USA	25	40	0.48	OK	Need
3.	VLBA_HN	USA	25	32	0.48	OK	Need
4.	VLBA_NL	USA	25	30	0.49	OK	Need
5.	VLBA_FD	USA	25	30	0.55	OK	Need
6.	VLBA_LA	USA	25	30	0.50	OK	Need
7.	VLBA_PT	USA	25	30	0.52	OK	Need
8.	VLBA_KP	USA	25	30	0.55	OK	Need
9.	VLBA_OV	USA	25	25	0.47	OK	Need
10.	VLBA_BR	USA	25	30	0.50	OK	Need
11.	VLBA_MK	USA	25	27	0.45	OK	Need
12.	Algonquin	Canada	46			Need upgrade	Need
13.	Usuda	Japan	70			Need upgrade	Need
14.	Kashima	Japan	34			Need upgrade	OK
15.	Nanshan	China	25			Need upgrade	OK
16.	Sheshan	China	25			Need upgrade	OK
17.	Mopra	Australia	22	36	0.60	OK	Need
18.	Parkes	Australia	64			Need upgrade	Need
19.	Hobart	Australia	26			Need upgrade	Need
20.	Ceduna	Australia	30			Need upgrade	Need

Twenty radio telescopes listed in Table 4.1 are operated under different conditions of access for external users. Those listed in rows 1 – 11 and 17 – 20 (light blue shadow) operate as opened facilities available to the world-wide scientific community on the basis of peer-reviewed scientific proposal. Such the proposals, requesting observational resources needed for the Huygens VLBI experiment on 14 January 2005 and two observing test sessions in July and October 2004, have been submitted by the Huygens VLBI team to the appropriate programme committees in Australia, USA and Europe in January – February 2004. Results of their evaluation are expected in March-April 2004.

Radio telescopes listed under No. 15–16 (light yellow shadow) are members of the European VLBI Network (EVN) and operate as open scientific facilities as well. However, there will be no observing EVN session in January 2005. Therefore, participation of these two radio telescopes in China must be arranged specially. The JIVE Huygens team is in contact with the administration and staff of these telescopes.

Radio telescopes listed under No. 12–14 are operated as private or non-open facilities. Their involvement in the Huygens tracking experiment must be arranged under special

separate agreements with appropriate organizations. The JIVE Huygens team has well established contacts with these organizations, but additional support from ESA might be required.

In order to participate in Huygens VLBI tracking, radio telescopes must be equipped with two critical devices – a receiver capable to observe at 2040 MHz and a VLBI Mk5 data acquisition system. Status of these two components as of January 2004 is listed in the last two columns of Table 4.1. Details of the engineering solutions for upgrade needed for the S-band receivers and data acquisition systems vary between different telescopes and are subject of intensive consultations between the JIVE team and appropriate observatories. Budgetary request based on these consultations is presented in Annex 1. We note that equipping radio telescopes with Mk5 data acquisition systems is required in order to process data using both wide-band signal from the reference celestial sources and narrow-band signal from the probe.

4.2. Data processing equipment

As described in [1], data processing of the Huygens tracking experiment will require a "standard" Mk4 wide band correlator and a purpose-built narrow band VLBI toolkit, the so called Huygens VLBI toolkit. The former, the EVN Mk4 Data Processor, is available at JIVE. As an operational element of the European VLBI Network it is an open scientific facility, available on the basis of peer-reviewed scientific proposals. Such the proposal has been submitted to the EVN Programme Committee in January 2004 (alongside with the requests for radio telescopes). A response from the Programme Committee is expected in March-April 2004. Development of the Huygens software toolkit has begun under the current project (see Section 3 of this Report). Resources needed for its future development as well as manpower, required for post-correlation processing and analysis of the Huygens VLBI tracking data are described in Annex 1.

4.3. Major milestones toward "live" Huygens VLBI tracking observations

The study, described in this report, resulted in (a) development and tests of the Huygens VLBI tracking software model toolkit and (b) preparatory radio astronomy observations of the Huygens Field. Further milestones toward "live" Huygens VLBI observations must include:

1). Implementation of the Huygens VLBI tracking software toolkit on the appropriate multi-processor platform, such as a LINUX PC-cluster.

2). Completion of the "reconnaissance" radio astronomy study of the Huygens Field by the data reduction of the EVN observations conducted in February 2004. This step will complete the data-base on the celestial reference sources in the Huygens Field and will allow us to make the choice of appropriate phase calibrators.

3). Test VLBI observations with the telescopes which will participate in "live" Huygens observations. Given complexity and non-standard character of the observing setup, at

least two such full-scale tests ("drills") must be conducted, approximately 6 and 3 months prior to the interface epoch, i.e. in July-August and October 2004. Observing proposals, described in Section 2 do include requests for such the test runs.

Budgetary and logistical considerations described in Annex 1 correspond to the three milestones above.

5. Conclusions

In the framework of the study described in this report we have confirmed feasibility of detection and VLBI tracking of the Huygens Probe's S-band signal by a network of Earth-based radio telescopes. This study is based on and continues the work described in [1]. Specific results of the present stage of the Huygens VLBI tracking project are:

1. An extensive campaign of radio astronomy reconnaissance of the Huygens Field has been conducted in the period November 2003 – February 2004, using ATCA, WSRT, VLA, MERLIN and EVN. A catalog of background radio sources – candidates for phase-referencing calibration of the Huygens S-band signal has been created (Appendix B). Several most compact sources in the close vicinity of the interface point has been observed with VLBI (EVN), their properties (radio structures) will be used in the phase-referencing process of the Huygens signal.

2. Algorithms of signal processing for the weak probe's signal have been implemented in the so-called Huygens VLBI software toolkit. The latter was tested on real data obtained in the EVN observations and an attempt to detect UHF signal from Beagle 2 using the Westerbork Synthesis Radio Telescope on 26 December 2003. The algorithms are now ready for implementation on a powerful cluster of processors for handling real Huygens data.

3. Twenty radio telescopes in the Pacific area have been contacted by various means (via peer-reviewed proposals or directly) in order to create a network for Huygens VLBI tracking. Technical readiness of the potential network has been investigated. This investigation created a basis for the programmatic and logistical request described in Annex 1.

4. A series of milestones for the period March 2004 – January 2005 aimed toward "live" Huygens VLBI observations has been established (section 4.3).

6. Acknowledgements

We express our gratitude to the directors and staff of the Australia Telescope National Facility, Westerbork Radio Observatory, Very Large Array of the National Radio Astronomy Observatory (a facility of the National Science Foundation operated under a cooperative agreement by Associated Universities, Inc.) and MERLIN (a national facility operated by the University of Manchester at Jodrell Bank Observatory on behalf of PPARC) for their support to the observations described in this report. We are particularly grateful to R.Sault (ATNF), A.Foley (ASTRON), T.Maxlow and P.Thomassen (MERLIN) for conducting observations and assisting in data reduction, and M.Garrett, H.J. van Langevelde and S.Parsley for useful discussions.

7. References

[1] VLBI Observations of the Huygens Probe, JIVE Research Note #0004, 10 Jul 2003

[2] Schilizzi R.T., Aldrich W., Anderson B., Bos A., Campbell R.M., Canaris J., Cappallo R., Casse J.L., Cattani A., Goodman J., van Langevelde H.J., Maccafferri A., Millenaar R., Noble R.G., Olnon F., Parsley S.M., Phillips C., Pogrebenko S.V., Smythe D., Szomoru A., Verkouter H., Whitney A.R., 2002, "The EVN-MarkIV VLBI Data Processor", Experimental Astronomy 12, 49

[3] Whitney A.R., 2003, "Mark 5 Disk-based Gbps VLBI Data System", in New technologies in VLBI, ed. Y.C.Minh, ASP Conf Series, v. 306, 123

[4] Koyama Y., 2002, International eVLBI experiments, www2.crl.go.jp/ka/radioastro/tdc/news_21/pdf/kovama.pdf

[5] Whitney A. 2000, MarkIIIA/IV/VLBA Tape Formats, Recording Modes and Compatibility, MkIV Memo #230.3

[6] Cassini/Huygens, Integrated Data Report, ESA-JPL-HUY-25999, 30 Nov 2002

[7] Pogrebenko S.V., Gurvits L.I., Campbell R.M., Avruch I.M., Lebreton J.-P., van't Klooster C.G.M., 2004, "VLBI tracking of the Huygens probe in the atmosphere of Titan", in Planetary Probe Atmospheric Entry and Descent Trajectory Analysis and Science, ed. A.Wilson, ESA SP-544, 197--204

ATCA Survey of the Huygens Field at 2.4 GHz
(see details in Section 2.1)

Designation	RA (J2000)	Dec (J2000)	I_{peak} [mJy/bm]	S_{tot} [mJy]	s_S [mJy]	Axes [mas]	
						Major	**Minor**
1	2	3	4	5	6	7	8
ATCA 1	07 39 41.66	21 32 28.30	9.2	13.2	0.98	20.0	9.5
ATCA 2	07 39 44.72	20 53 46.13	145.9	297.2	9.24	11.0	22.9
ATCA 3	07 39 52.13	20 55 26.48	126.4	171.1	5.68	6.4	14.6
ATCA 4	07 39 56.33	21 30 43.66	12.5	14.1	0.54	9.1	7.4
ATCA 5	07 40 04.01	21 14 53.03	6.0	42.5	1.47	91.6	31.1
ATCA 6	07 40 10.39	21 38 14.33	4.6	6.3	0.63	12.1	11.9
ATCA 7	07 40 11.13	21 13 12.03	5.0	8.4	0.95	28.2	9.1
ATCA 8	07 40 12.23	21 37 23.33	1.9	5.7	0.41	39.4	12.5
ATCA 9	07 40 19.18	21 01 32.08	5.6	10.8	0.50	26.9	15.2
ATCA 10	07 40 20.17	21 38 45.82	3.1	4.6	0.58	27.0	5.9
ATCA 11	07 40 28.46	21 37 34.89	7.4	9.0	0.35	12.3	7.2
ATCA 12	07 40 34.39	21 13 38.95	3.2	4.0	0.51	21.3	2.0
ATCA 13	07 40 39.47	21 11 25.52	2.6	8.3	0.34	55.1	17.5
ATCA 14	07 40 43.37	20 58 53.90	28.2	31.3	0.37	7.6	5.1
ATCA 15	07 40 46.88	20 44 04.46	15.5	17.4	0.93	13.6	0
ATCA 16	07 41 05.69	21 16 43.17	2.4	4.5	0.30	29.9	13.3
ATCA 17	07 41 07.76	20 46 14.65	2.7	3.9	0.37	47.4	4.2
ATCA 18	07 41 10.65	20 59 45.54	2.5	3.0	0.22	21.6	2.4
ATCA 19	07 41 11.35	21 46 38.61	2.3	2.6	0.43	5.3	5.9
ATCA 20	07 41 11.36	21 11 43.25	8.7	11.3	0.31	9.5	11.4
ATCA 21	07 41 13.05	21 05 44.34	1.3	6.8	0.32	81.4	21.3
ATCA 22	07 41 19.13	20 50 26.68	61.4	80.0	0.79	14.7	8.6
ATCA 23	07 41 20.23	22 00 53.28	17.4	23.3	1.25	28.4	4.6
ATCA 24	07 41 20.33	20 51 18.35	73.3	99.6	1.37	9.6	8.5
ATCA 25	07 41 21.27	20 53 22.51	4.4	4.8	0.29	13.4	7.1
ATCA 26	07 41 27.51	20 43 35.46	6.0	9.2	0.77	49.3	7.9
ATCA 27	07 41 30.91	20 59 01.50	1.5	1.3	0.37	0	0
ATCA 28	07 41 33.78	21 14 29.21	2.6	3.6	0.34	31.2	2.1
ATCA 29	07 41 35.71	20 48 44.68	2.0	3.9	0.41	22.4	17.6
ATCA 30	07 41 40.62	21 16 41.89	39.3	45.2	0.43	4.8	8.2
ATCA 31	07 41 42.22	21 16 43.22	21.1	25.9	0.40	9.0	7.8
ATCA 32	07 41 47.02	20 59 43.39	1.8	4.3	0.26	57.4	8.2
ATCA 33	07 41 49.88	21 00 28.24	2.3	3.2	0.24	30.0	3.1
ATCA 34	07 41 58.00	22 04 02.41	7.1	18.4	0.48	36.4	13.7
ATCA 35	07 42 01.73	21 04 19.42	16.9	18.9	0.27	7.5	5.0
ATCA 36	07 42 04.86	21 32 14.88	13.0	13.6	0.24	11.3	1.5
ATCA 37	07 42 05.24	21 35 05.16	3.3	3.7	0.24	21.7	4.7
ATCA 38	07 42 08.76	20 58 03.45	1.8	2.0	0.24	22.7	3.5
ATCA 39	07 42 11.16	21 28 25.22	4.0	4.3	0.27	13.4	1.7

ATCA Survey of the Huygens Field at 2.4 GHz (cntd)

1	2	3	4	5	6	7	8
ATCA 40	07 42 20.94	20 52 42.72	18.6	22.2	0.39	15.3	6.1
ATCA 41	07 42 23.46	21 09 48.03	1.6	2.1	0.33	43.7	0
ATCA 42	07 42 31.95	21 58 05.18	2.2	2.0	0.24	6.1	0
ATCA 43	07 42 37.34	21 06 18.02	1.6	2.5	0.26	7.6	14.3
ATCA 44	07 42 41.58	21 27 29.25	1.6	2.1	0.30	17.0	6.9
ATCA 45	07 42 42.40	21 14 06.69	3.8	4.9	0.23	13.8	9.8
ATCA 46	07 42 51.35	21 14 02.10	4.9	7.6	0.22	12.8	9.8
ATCA 47	07 42 57.66	22 02 51.36	3.1	5.3	0.45	42.9	2.8
ATCA 48	07 43 12.69	21 02 42.20	51.7	82.3	0.57	9.3	12.8
ATCA 49	07 43 16.14	21 03 02.39	73.0	117.0	0.54	8.2	14.7
ATCA 50	07 43 18.41	21 46 47.79	2.2	2.3	0.28	10.0	0
ATCA 51	07 43 33.41	21 10 04.23	1.8	5.9	0.27	64.6	15.7
ATCA 52	07 43 39.78	21 44 55.99	1.4	1.0	0.25	3.9	0
ATCA 53	07 43 45.46	21 10 08.70	3.2	4.2	0.23	19.3	7.5
ATCA 54	07 43 47.55	21 44 18.56	6.7	8.9	0.27	18.5	10.0
ATCA 55	07 43 48.01	21 45 48.47	9.2	8.8	0.26	6.1	0
ATCA 56	07 43 53.11	21 31 52.34	4.4	7.1	0.35	20.3	4.8
ATCA 57	07 43 53.51	21 31 57.05	7.3	35.2	0.33	34.6	19.9
ATCA 58	07 43 53.75	21 32 01.58	13.7	28.6	0.46	27.3	17.7
ATCA 59	07 43 56.43	21 42 42.42	1.9	4.8	0.41	61.5	16
ATCA 60	07 43 56.53	21 44 03.93	1.7	4.0	0.36	70.8	12.5
ATCA 61	07 43 58.51	21 43 12.49	6.4	7.6	0.26	20.1	4.1
ATCA 62	07 44 01.20	20 58 33.15	8.2	8.4	0.34	12.4	0
ATCA 63	07 44 10.23	20 46 48.18	22.6	43.6	3.36	55.0	0
ATCA 64	07 44 30.72	21 45 27.82	1.9	12.2	0.42	156.9	25.4
ATCA 65	07 44 34.06	21 11 51.97	3.0	3.9	0.30	29.4	0.6
ATCA 66	07 44 47.27	21 20 01.21	64.2	64.9	0.66	5.5	1.4
ATCA 67	07 44 51.37	21 45 58.09	5.3	7.2	0.49	17.7	4.4
ATCA 68	07 44 55.73	21 38 33.17	13.0	41.3	0.72	14.8	19.8
ATCA 69	07 44 59.56	21 25 19.21	17.2	49.0	2.64	63.7	28.3
ATCA 70	07 44 59.59	21 28 40.73	3.7	6.9	0.41	51.1	4.8
ATCA 71	07 44 59.74	21 25 20.08	11.4	14.4	0.43	21.3	4.9
ATCA 72	07 45 08.32	21 27 02.88	3.5	7.5	0.54	64.6	6.7
ATCA 73	07 45 16.56	21 34 45.80	2.8	5.7	0.35	42.7	14.0
ATCA 74	07 45 18.70	21 36 57.45	1.7	2.8	0.32	44.6	10.0
ATCA 75	07 45 25.48	21 40 58.09	3.8	6.1	0.45	19.3	12.9
ATCA 76	07 45 26.88	21 41 53.20	2.3	9.8	0.38	79.4	20.6
ATCA 77	07 45 29.45	21 22 49.34	7.1	6.9	0.57	12.3	0
ATCA 78	07 45 30.02	21 15 32.41	29.3	31.4	0.75	7.5	4.5
ATCA 79	07 45 35.19	21 37 36.21	14.4	15.5	0.51	9.4	4.0

Catalog of radio sources in the Huygens Field (see Section 2 for details)

Source	Designation	RA (2000)	DEC (2000)	D(arc min)	Band	Instrument	Flux dens (pk/tot)	map_rms (uJy)	comments
	2	3	4	5	6	7	8	9	10
1	0742212X_2	07 42 49.41349	21 21 40.0002	2.30	X	VLA	0.28/0.7	78	diffuse,this is core
2	0742212X_3	07 42 54.70296	21 23 56.1002	3.43	X	VLA	1.6/2.0	75	
2	FLD-CEN-C_3	07 42 54.52306	21 23 55.8912		C	VLA	1.3/1.7	75	DBCON; "2" undetcd
3	07422127_1	07 42 41.59469	21 27 24.8996	4.63	X	VLA	1.62/1.7	93	"1"
3	07422126_1	07 42 41.44326	21 27 24.5977		C	VLA	0.61/.8	77	
3	ATCA 44	07 42 41.58	21 27 29.25		S	ATCA	1.6/2.1		
3	FIRST 204	07 42 41.686	21 27 25.11		L	FIRST	1.34/1.57		
4	0742211X_A	07 42 42.37534	21 14 04.0205	8.73	X	VLA	2.1/2.7	165	
4	07422114_A	07 42 42.41076	21 14 04.1344		C	VLA	2.6/4.0	227	
4	ATCA 45	07 42 42.40	21 14 06.69		S	ATCA	3.8/4.9		
4	FIRST 205	07 42 42.385	21 14 04.17		L	FIRST	5.05/5.50		
5	07422133_A	07 42 04.87587	21 32 13.9280	12.61	X	VLA	7.7/10.4	287	relook
5	07422131_A	07 42 04.88159	21 32 13.7982		C	VLA	9.0/10.4	194	
5	0739+216	07 42 04.87814	21 32 14.0400		C	MERLIN	7.0/6.7	120	unres
5	ATCA 36	07 42 04.86	21 32 14.88		S	ATCA	13.0/13.6		
5	FIRST 181	07 22 04.889	21 32 13.94		L	FIRST	15.01/15.32		
6	0740+216	07 43 53.72839	21 32 00.6000	19.31	C	MERLIN	0.8/1.0	112	weak; part resolved
6	FIRST 249	07 43 53.744	21 32 00.58		L	FIRST	21.19/22.68		core of core-dbl
6	ATCA ??					ATCA			ATCA 56-57-58 confsd
6	WSRT 24	07 43 53.61	21 32 09.20		U	WSRT	48.4		cnfsd
7	7432103	07 43 14.33148	21 02 49.4988	21.44	X	VLA	4.2/4.8	262	VLA arch AC406; core of core-dbl
7	0740+211	07 43 14.37161	21 02 49.8150		C	MERLIN	1.2/1.0	125	weak; core of FIRST dbl
7	FIRST 219	07 43 15.183	21 02 52.48		L	FIRST	6.54/104.72		confused?
8	0738+213	07 41 11.32280	21 11 44.8250	23.59	C	MERLIN	0.5/0.8	105	wk det; resolved?
8	ATCA 20	07 41 11.36	21 11 43.25		S	ATCA	8.7/11.3		
8	FIRST 128	07 41 11.423	21 11 43.28		L	FIRST	10.56/16.73		

	2	3	4	5	6	7	8	9	10
9	07432144_B	07 43 58.53768	21 43 13.2790	27.28	C	VLA	1.3/2.9	212	1of3comps
9	ATCA 61	07 43 58.51	21 43 12.49		S	ATCA	6.4/7.6		
9	FIR 253	07 43 58.537	21 43 13.25		L	FIRST	10.92/14.02		
10	07432145_A	07 43 48.02186	21 45 48.6487	27.82	X	VLA	3.6/5.5	193	steep sp?
10	07432144_A	07 43 48.03036	21 45 47.6761		C	VLA	5.5/7.8	216	
10	ATCA 55	07 43 48.01	21 45 48.47		S	ATCA	9.2/8.8		
10	FIRST 246	07 43 48.014	21 45 48.25		L	FIRST	9.08/9.28		
11	0744211X_A	07 44 47.27881	21 20 00.4324	29.58	X	VLA	39.9/41.3	164	
11	07442119_A	07 44 47.27512	21 20 00.4461		C	VLA	49.6/50.9	211	
11	0741+214	07 44 47.27720	21 20 00.4050		C	MERLIN	33.6/34.3	240	deep hole NW side src
11	ATCA 66	07 44 47.27	21 20 01.21		S	ATCA	64.2/64.9		
11	FIRST 291	07 44 47.289	21 20 00.31		L	FIRST	74.72/78.15		
11	WSRT 29	07 44 47.25	21 20 21.29		U	WSRT	47.3		840MHz
12	07442057_A	07 44 01.22240	20 58 33.9803	30.63	X	VLA	6.8/7.3	171	no C obs
12	ATCA 62	07 44 01.20	20 58 33.15		S	ATCA	8.2/8.4		
12	FIRST 257	07 44 01.232	20 58 33.81		L	FIRST	8.71/8.79		
13	0736+216	07 39 56.35286	21 30 43.8850	39.08	C	MERLIN	5.5/5.8	131	unresolved(JMFIT)
13	ATCA 4	07 39 56.33	21 30 43.66		S	ATCA	12.5/14.1		
13	FIRST 70	07 39 56.359	21 30 43.78		L	FIRST	13.90/14.75		
14	0742+215A	07 45 29.44504	21 22 48.6650	30.26	C	MERLIN	0.67/1.4	104	weak; resolved?
14	ATCA 77	07 45 29.45	21 22 49.34		S	ATCA	7.1/6.9		
14	FIRST 321	07 45 29.440	21 22 48.77		L	FIRST	12.66/14.18		
14	WSRT 32	07 45 29.30	21 22 35.72		U	WSRT	18.7		
15	0742+213	07 45 30.02058	21 15 31.2200	40.08	C	MERLIN	1.1/1.0	113	weak; unres?
15	ATCA 78	07 45 30.02	21 15 32.41		S	ATCA	29.3/31.4		
15	FIRST 322	07 45 30.043	21 15 31.28		L	FIRST	43.85/50.01		
15	WSRT 33	07 45 29.96	21 15 14.39		U	WSRT	51.2		

	2	3	4	5	6	7	8	9	10
16	0738+221	07 41 20.19236	22 00 54.9000	42.47	C	MERLIN	4.3/6.3	116	partial resolved
16	ATCA 23	07 41 20.23	22 00 53.28		S	ATCA	17.4/23.3		
16	FIRST 139	07 41 20.190	22 00 54.86		L	FIRST	27.68/28.12		
16	WSRT 22	07 41 20.15	22 01 06.98		U	WSRT	32.6		
17	0742+217	07 45 35.20820	21 37 36.3700	43.19	C	MERLIN	7.1/7.4	130	
17	ATCA 79	07 45 35.19	21 37 36.21		S	ATCA	14.4/15.5		
17	FIRST 327	07 45 35.217	21 37 36.36		L	FIRST	19.62/20.94		
18	0732+207	07 35 52.74311	20 36 38.8270	105.8	C	MERLIN	203.5/204.5	1020	unresolved(JMFIT)